nature photonics

LETTERS

PUBLISHED ONLINE: 12 MAY 2013 | DOI: 10.1038/NPHOTON.2013.102

Experimental boson sampling

Max Tillmann[1,2]*, Borivoje Dakić[1], René Heilmann[3], Stefan Nolte[3], Alexander Szameit[3] and Philip Walther[1,2]*

Universal quantum computers[1] promise a dramatic increase in speed over classical computers, but their full-size realization remains challenging[2]. However, intermediate quantum computational models[3–5] have been proposed that are not universal but can solve problems that are believed to be classically hard. Aaronson and Arkhipov[6] have shown that interference of single photons in random optical networks can solve the hard problem of sampling the bosonic output distribution. Remarkably, this computation does not require measurement-based interactions[7,8] or adaptive feed-forward techniques[9]. Here, we demonstrate this model of computation using laser-written integrated quantum networks that were designed to implement unitary matrix transformations. We characterize the integrated devices using an *in situ* reconstruction method and observe three-photon interference[10–12] that leads to the boson-sampling output distribution. Our results set a benchmark for a type of quantum computer with the potential to outperform a conventional computer through the use of only a few photons and linear-optical elements[13].

More than a decade ago, Knill, Laflamme and Milburn (KLM) showed in their seminal work[14] that scalable photonic quantum computing is possible using only linear optical circuits, single-photon sources and detectors, and measurement-induced effective nonlinearities. The use of ancillary photons not only enables the heralding of successful gate operations[7,8], but also provides a basis for protocols in which probabilistic two-photon gates are teleported into a quantum circuit with high probability[15]. Despite impressive theoretical progress[16–19], the number of indistinguishable ancilla photons required for a universal optical quantum computer appears to be very challenging given current photonic quantum technology[20].

Several interesting intermediate models of quantum computation have been proposed recently[3–5]. Although they do not enable universal quantum computation, these models still provide a dramatic increase in computational speed for particular tasks. In contrast to the proposed KLM scheme, these models need neither entangling gate operations, adaptive measurements, nor ancilla photons, and are thus technically more feasible. The intermediate quantum computation model proposed by Aaronson and Arkhipov[6] seems to be extremely resource-efficient, as it utilizes the unique advantages of the mobility and bosonic nature of photons to solve the so-called sampling problems that are believed to be classically hard[13,21]. In general, sampling problems ask for random samples according to a specified probability distribution. The probability distributions and how they are specified depend on the problem class, such as the boson sampling problem considered in our work.

Here, we experimentally solve small instances of the boson-sampling problem by implementing Aaronson and Arkhipov's model of computation with non-interacting bosons, specifically photons. Randomly chosen instances of this problem are strongly believed to be hard to solve by classical means. Instances of boson sampling can be realized with quantum systems composed of non-interacting photons that are processed through randomly chosen networks of physical modes. The bosonic nature of the photons leads to non-classical interference, producing an output

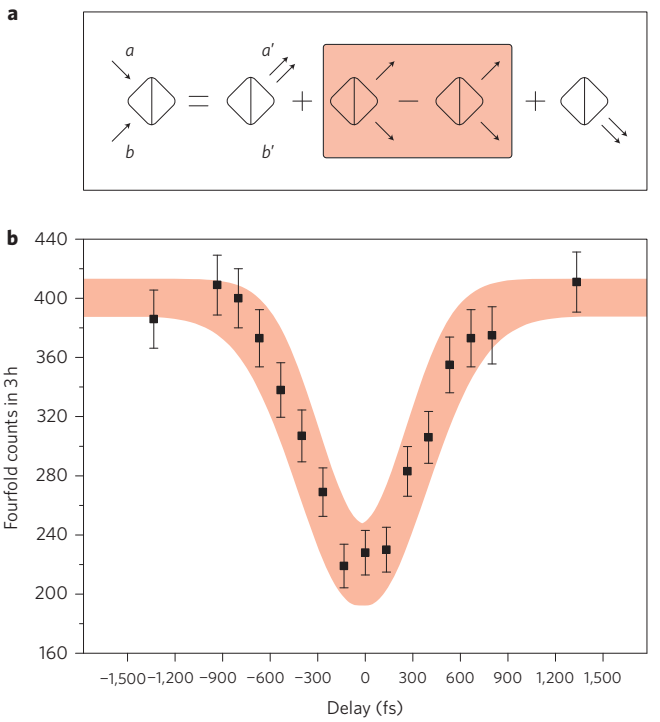

Figure 1 | Non-classical interference. a, Basic two-photon interference. When two indistinguishable photons enter a 50/50 beamsplitter, destructive interference of having both photons either transmitted or reflected (highlighted) leads to bunching such that both photons must be found together in one of the two output modes a' or b'. Therefore, the probability of finding two photons in different output modes is zero. This is described mathematically as the permanent of the 50/50 beamsplitter unitary. **b**, Example of experimental three-photon interference. Three photons were injected into input modes 3, 4 and 5 of one of our optical networks. We measured fourfold coincidence counts between a trigger detector and output modes 2, 4 and 5 of our device, while simultaneously delaying the input photons in modes 4 and 5. The dip shows a clear signature of genuine three-photon interference. The error for the experimental data follows a Poissonian distribution of the measured counts. The shaded area represents the Gaussian fit including errors.

[1]Faculty of Physics, University of Vienna, Boltzmanngasse 5, A-1090 Vienna, Austria, [2]Institute for Quantum Optics and Quantum Information, Austrian Academy of Sciences, Boltzmanngasse 3, A-1090 Vienna, Austria, [3]Institute of Applied Physics, Abbe Center of Photonics, Friedrich-Schiller Universität Jena, Max-Wien-Platz 1, D-07743 Jena, Germany. *e-mail: max.tillmann@univie.ac.at; walther-office@univie.ac.at

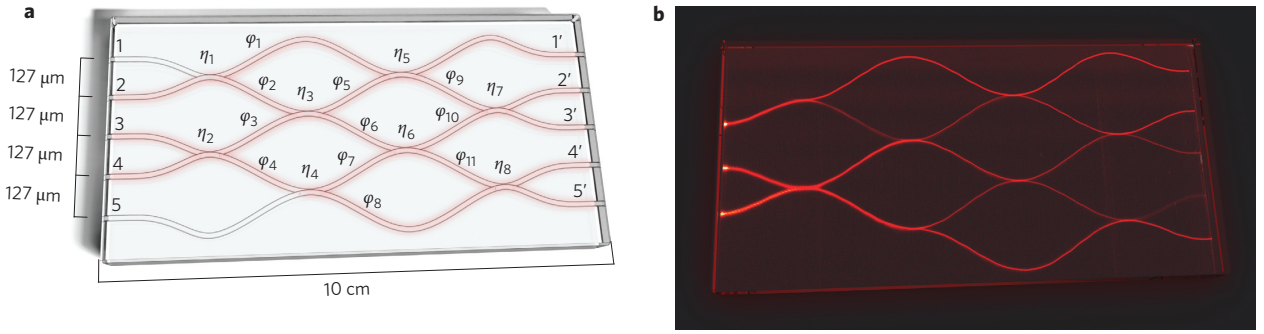

Figure 2 | The optical networks. a, Schematic. The circuit consists of five input modes (1 to 5), five output modes (1′ to 5′), eight directional couplers (η_1 to η_8) and eleven phase shifters (φ_1 to φ_{11}). Up to three single photons can be coherently launched into any combination of input modes. Each output mode is connected to a single-photon detector, and coincidences are recorded with a home-built FPGA logic. Neighbouring modes are separated by 127 μm and the chip has a total length of 10 cm. Three different optical networks written on the same chip were used in the experiment. **b**, Fluoresence image. To visualize the light evolution in the network, coherent laser light at a wavelength of 633 nm was launched into input modes 2 to 4 of an optical network. Colour centres are excited by the propagating beam and emit fluorescent light at a wavelength of 650 nm. The fluoresence signal is directly proportional to the propagating light intensity.

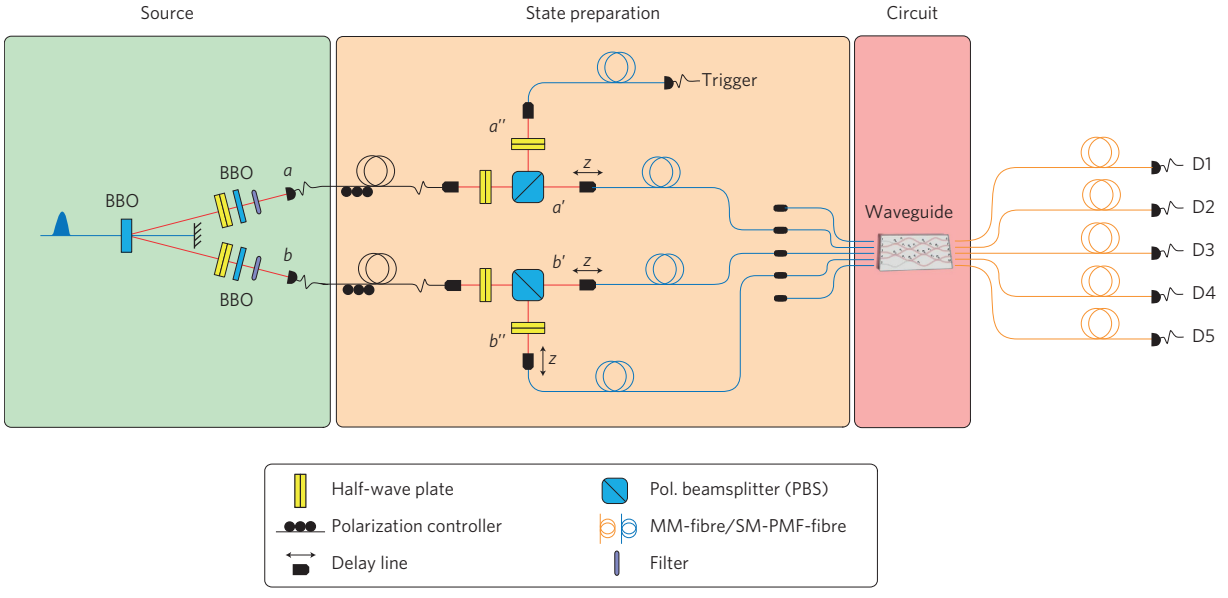

Figure 3 | Experimental set-up. The experimental set-up can be divided into three main parts. The first part is a downconversion source pumped with 150 fs pulses at a wavelength of 394.5 nm and c.w.-equivalent power of 700 mW. Four photons are created using higher-order emissions from a 2 mm BBO crystal cut for a non-collinear type II process. Filtering with $\lambda_{FWHM} = 3$ nm filters guarantees spectral indistinguishability. Two HWPs and two 1 mm BBO crystals are used for the correction of birefringent walk-off effects. The photons are coupled to single-mode fibres and guided to the state preparation stage. Here, fourfold events are split up via two PBSs, and a HWP in mode b'' ensures that all photons entering the integrated device exhibit the same polarization. The input photons are coupled into polarization-maintaining fibres (PMFs) that can be mated to any of the five fibres of the input fibre array. Temporal overlap in the circuit is achieved with three delay lines. After passing through the waveguide, the photons are coupled to graded-index multimode fibres and sent to single-photon avalanche photodiode detectors (D1 to D5).

probability distribution for which there is no known efficient classical sampling algorithm. The simplest case of the non-classical interference effect has been demonstrated for two photons by Hong, Ou and Mandel (HOM)[22].

When two indistinguishable photons enter a 50/50 beamsplitter from different input modes, a and b, the two photons will always end up propagating together in one of the two output modes (Fig. 1a). This occurs because a 50/50 beamsplitter represents a unitary transformation[23] that cancels the probability of having both photons transmitted with the probability of having both photons reflected. More generally, the probability of finding one photon in output mode a' and the other in mode b' is given by the permanent (see Methods) of the beamsplitter matrix BS:

$$P = |\mathrm{Per(BS)}|^2 = \left|\mathrm{Per}\begin{pmatrix} T & iR \\ iR & T \end{pmatrix}\right|^2 = |T^2 - R^2|^2$$

where T and R are beamsplitter transmission and reflection coefficients, respectively. In the case of a 50/50 beamsplitter the permanent is obviously zero, so the photons bunch into one of the output modes. The same formula holds for the general case of n photons injected into n different modes of an $m \times m$ optical network with a underlying matrix U. The probability that one finds these

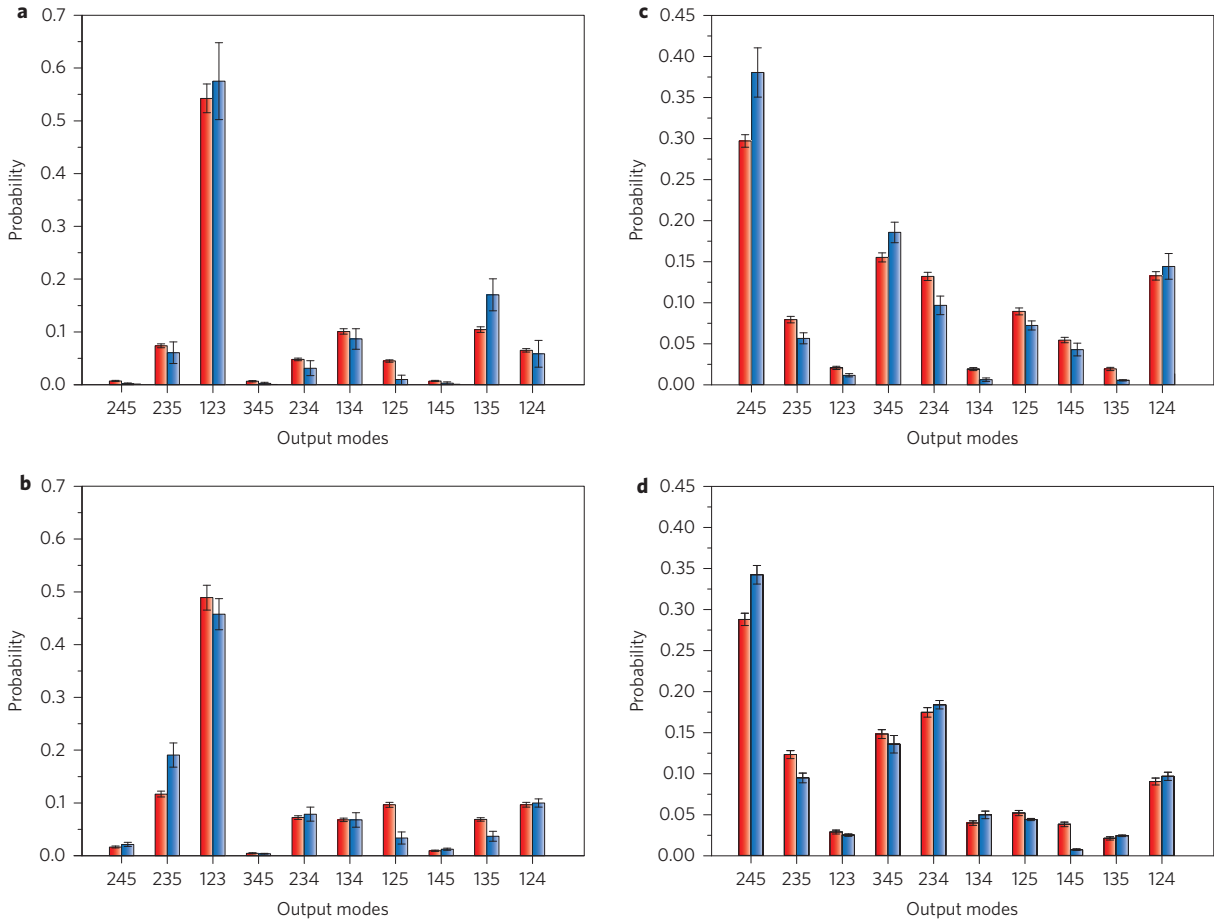

Figure 4 | Three-photon probabilities. a–d, Experimentally measured (red) and theoretical (blue) three-photon probabilities for the ten possible output combinations. Photons were injected into input modes 1, 2 and 4 of device no. 1 (**a**) and device no. 2 (**b**), and input modes 3, 4 and 5 of device no. 2 (**c**) and device no. 3 (**d**). These input modes were chosen for experimental reasons. The errors for the probabilities follow a Poissonian distribution. For the measured output distributions, we obtain fidelities F (see Supplementary Information for definition of the fidelity) of 0.98 ± 0.01 (**a**), 0.97 ± 0.01 (**b**), 0.98 ± 0.01 (**c**) and 0.96 ± 0.01 (**d**).

photons in different n output modes is given by the permanent of the $n \times n$ submatrix $\tilde{U}$ of the unitary U, $P = |\mathrm{Per}(\tilde{U})|^2$ (see Methods). For complex networks, such as randomly designed networks, computing the permanent of the underlying unitary matrix on a classical computer is conjectured to scale exponentially in time[6] with respect to the size of the unitary matrix. Thus, even for today's most powerful conventional computers, this puts an upper limit on the size of a unitary matrix for which the output distribution can be sampled. It was estimated that for a random optical network of $n \approx 20$ photons in $m \approx 400$ modes, sampling the output distribution is already intractable for conventional computers[13].

Even though bosons tend to bunch, a phenomenon also known as the 'boson birthday paradox'[24], for networks with a sufficiently large number of modes ($m \gg \sqrt{n}$), the probability of detecting n photons in n spatially separated modes as n-fold coincidences dominates. This remarkable feature reduces the technological requirements, as no number-resolving detectors are needed for this intermediate model of quantum computation, thereby making a fully fledged boson-sampling computation more feasible in the near future. Therefore, in our experiment we consider only those measurement outcomes where three photons are detected in spatially separated modes.

The boson-sampling computation is demonstrated for different randomly designed optical networks. The computation is initialized by the insertion of three indistinguishable photons, one in each input mode, into an integrated circuit with five input and five output modes. After propagation through the waveguide structures, the output distribution is recorded.

Each integrated circuit was fabricated with a direct laser-writing technique[25,26] and consists of five spatial modes coupled by eight beamsplitters and eleven phase shifters (Fig. 2 and Supplementary section, 'Reconstruction'). We randomly generated our beamsplitting ratios and phases on a classical computer as a guideline for chip fabrication (Supplementary section, 'Fabrication'). To obtain different optical networks, two parameters were varied during the fabrication process: the phases, by adjusting the relative path length between optical elements, and the beamsplitter ratios, by tuning the evanescent coupling among the modes. To ensure that the sampling of bosons is classically hard to simulate, the underlying unitary matrix needs to be of sufficient complexity. Here, the randomization of the beamsplitting ratios and phase shifts ensures the desired complexity. An arbitrary 5×5 unitary matrix requires, in principle, access to 25 independent parameters for a full specification[27]. In our experiment, we use networks with 19 randomized parameters on three photons, a scenario that demonstrates sufficient complexity for our benchmark realization of boson sampling.

The three-photon input state was generated via the process of spontaneous parametric downconversion[28]. To enable a heralded three-photon emission into well-defined modes, a double-pair emission of entangled photons was utilized. The photon source

was aligned to emit the entangled state $|\Phi^+\rangle = (|H\rangle_a|H\rangle_b + |V\rangle_a|V\rangle_b)/\sqrt{2}$, where H and V denote horizontal and vertical polarizations, respectively, and a and b correspond to the two spatial modes. With 700 mW continuous-wave (c.w.) equivalent pump power, two photon pairs are also emitted as a fourfold emission, while keeping the higher-order terms low. To enable a triggered three-photon emission, two photon pairs must be emitted simultaneously into spatial modes a and b, resulting in

$$|\Psi\rangle_{a,b} = \left(|HH\rangle_a|HH\rangle_b + |HV\rangle_a|HV\rangle_b + |VV\rangle_a|VV\rangle_b\right)/\sqrt{3}$$

These photons are guided to two polarizing beamsplitters (PBS1 and PBS2) such that a successful detection event in the trigger mode a'' heralds the generation of the states $|H\rangle_{a'}|H\rangle_{b'}|V\rangle_{b''}$ or $|VV\rangle_{b'}$. Post-selection on a fourfold coincidence, consisting of the trigger event and three detection events in the output modes of the circuit, ensures that three photons enter the waveguide in separate spatial modes. A half-wave plate (HWP) in mode b'' introducing a 90° rotation is used to render the photons indistinguishable in polarization. Using mating adapters, the three photons can be inserted in any combination of three input modes of the polarization-maintaining fibre array that is butt-coupled to the integrated device. A schematic of the experimental setup is shown in Fig. 3. Three delay lines are used to temporally overlap the photons for non-classical interference. The initial calibration was carried out by using two-photon input states. Operating the source at a reduced value of 200 mW c.w.-equivalent power, bright two-photon emission enabled high-precision alignment scans with good statistics. Non-classical interference between the first and second input modes was first optimized by adjusting the delay line for input mode two. Non-classical interference between the first and third input modes was then optimized by adjusting the delay line for input mode three. A final scan of the delay between input modes two and three was used as feedback for optimal temporal overlap of all three photons. This alignment was then verified for three-photon interference, where the laser source was operated at higher pump powers, by finely adjusting the delay lines for maximal non-classical interference. This ensures that the three non-interacting photons exhibit maximum indistinguishability. After successful calibration, the output probabilities were recorded for 20 h per setting.

The multiphoton interference on the chip[10] is controlled by three adjustable delay lines to temporally overlap the photons. Scanning the temporal delays results in a three-photon HOM dip that acts as a strong signature of the non-classical interference of the three photons (Fig. 1b). The underlying unitary operation of the integrated circuits was reconstructed by using an adaption of a recently proposed method[29]. For each optical network, the 19 parameters were fitted to the experimentally acquired 25 single-photon probabilities and 40 two-photon visibilities (see Methods). Although there might be symmetry in the circuit that could affect the fitting parameters, the global unitary remains the same. Figure 4 depicts the experimental data and theoretical predictions of the boson-sampling computation for two different integrated circuits. The output distributions are in good agreement with the theoretical values obtained from the reconstructed unitary matrices, as one can judge from the fidelities (above 95%; Fig. 4).

Our experiment presents the first benchmark quantum computation on randomly designed optical networks showing a boson-sampling computation. This intermediate model of quantum computation is of particular interest, because the bosonic interference of photons in random networks is already hard to simulate on conventional computers. In contrast to universal models of photonic quantum computers, the boson-sampling computation requires only passive optical elements. This relaxes the physical requirements significantly, so a continuous improvement in current multiphoton sources and detection efficiencies as well as reductions in the losses in integrated circuits might, in the near future, lead to quantum computations in regimes where classical verification is no longer possible.

Note that, during the review process of the work presented here, we learned of parallel experiments by Spring *et al.*[30], Broome *et al.*[31] and Crespi *et al.*[32].

Methods

Boson sampling computation. This intermediate model of quantum computation involves a quantum system of n non-interacting bosons operating between m physical modes, where $m > n$. We define the computation basis states $|i_1, i_2, \ldots, i_m\rangle$, where $i_1 + i_2 + \cdots + i_m = n$. For example, the state $|2, 1, 0, 1\rangle$ is the state of two bosons in the first mode and one boson in the second and fourth mode. The total number of states in the computational basis $D = \binom{m+n-1}{n}$ is exponentially large in m. As there is no interaction, all the gates in the model are single-particle transformations defined by $m \times m$ complex unitary matrices. For the purposes of this work it is important to recall the definition of the permanent of a $m \times m$ matrix U

$$\mathrm{Per}(U) = \sum_{\sigma \in S_m} \prod_{i=1}^{m} U_{i,\sigma(i)}$$

where S_m is the set of all permutation of m elements. For example, the permanent of 2×2 unitary matrix $U = \begin{pmatrix} a & b \\ c & d \end{pmatrix}$ reads $\mathrm{Per}(U) = ad + bc$. If the $m \times m$ matrix U exhibits sufficient complexity then the evaluation of its permanent is strongly believed to be hard on a classical computer. This means that the computation is inefficient (non-polynomial) in steps of computation in m. Consider an input state $|I\rangle = |i_1, i_2, \ldots, i_m\rangle$ of n bosons in m modes that is transformed via some unitary $m \times m$ matrix U. The probability of finding the state $|O\rangle = |j_1, j_2, \ldots, j_m\rangle$ at the output is given by

$$P_{I,O} = |\langle O|U \otimes U \ldots \otimes U|I\rangle|^2$$

Careful analysis[6] shows that this probability can be expressed trough the matrix permanents

$$P_{I,O} = \frac{|\mathrm{Per}(U_{I,O})|^2}{i_1!i_2!\ldots i_m!j_1!j_2!\ldots j_m!} \quad (1)$$

where the $n \times n$ matrix $U_{I,O}$ is defined in the following manner. First we define the $m \times n$ matrix U_I by taking i_k copies of the kth column of U, for each $k = 1, \ldots, m$. We then form the $n \times n$ matrix $U_{I,O}$ by taking j_k copies of the kth row of U_I, for each $k = 1, \ldots, m$. As an example, consider a 3×3 matrix

$$U = \begin{pmatrix} a & b & c \\ d & e & f \\ g & h & j \end{pmatrix}$$

and the input $|I\rangle = |1, 1, 0\rangle$ and output state $|O\rangle = |0, 1, 1\rangle$. Than the matrix U_I is

$$U_I = \begin{pmatrix} a & b \\ d & e \\ g & h \end{pmatrix}$$

and finally $U_{I,O}$ reads

$$U_{I,O} = \begin{pmatrix} d & e \\ g & h \end{pmatrix}$$

Therefore, the probability of finding state $|O\rangle = |0, 1, 1\rangle$ at the output, that is, to find one boson in mode 2 and one in mode 3, is given by

$$P_{I,O} = \frac{|\mathrm{Per}(U_{I,O})|^2}{1!1!0!0!1!1!} = |dh - eg|^2$$

From the previous example, it is clear that for cases where the input and output modes are occupied by at most one boson the matrix $U_{I,O}$ turns out to be the $n \times n$ submatrix of U.

The problem of sampling the output distribution given by equation (1) is called a bosonic sampling problem. Whereas a quantum realization (bosonic computer) solves the problem efficiently, it is strongly believed that it cannot be solved efficiently by a classical computer.

Experimental set-up. An 80 MHz Ti:sapphire oscillator (Chameleon, Coherent Inc.) emitting 150 fs pulses at 789 nm (2.5 W c.w.-equivalent power) is upconverted to 700 mW c.w.-equivalent power at 349.5 nm via a LiB_3O_5 crystal (LBO) (HarmoniXX, A.P.E GmbH). The beam is focused on a 2 mm β-BaB_2O_4 (BBO) crystal cut for degenerate non-collinear type-II spontaneous parametric downconversion[28]. To achieve spectral indistinguishability, the downconverted photons are filtered by interference filters ($\lambda_{FWHM} = 3$ nm) and collected with single-mode fibres. The c.w.-equivalent pump power of 700 mW allows for emission of fourfold states at high count rates. Noise contribution from higher-order terms was measured to be lower than 4%. The double-pair emission of the source generates the state

$$|\Psi\rangle_{a,b} = \left(|HH\rangle_a|HH\rangle_b + |HV\rangle_a|HV\rangle_b + |VV\rangle_a|VV\rangle_b\right)/\sqrt{3}$$

Two polarizing beamsplitters (PBS1 and PBS2) distribute the photons into four modes such that a fourfold coincidence post-selection guarantees that three photons enter the waveguide in different modes. HWPs ensure indistinguishability in polarization. Three delay lines are used to temporally overlap the photons for non-classical interference. The photons reach the integrated circuit via a polarization maintaining V-groove fibre array that is butt-coupled to the waveguide. Index-matching gel is applied to reduce reflection losses. A graded-index multimode fibre array is butt-coupled to the output of the waveguide and connected to single-photon avalanche photodetectors. Optimal coupling between the integrated device and the fibre arrays is achieved with two six-axis alignment stages. Coincidences are recorded with a home-built field-programmable gate array logic.

Chip fabrication. The waveguides were written inside high-purity fused silica (Corning 7980ArF grade) using a RegA 9000 seeded by a Mira Ti:sapphire femtosecond laser. The pulse duration was 150 fs at 800 nm with a repetition rate of 100 kHz and pulse energy of 200 nJ. The pulses were focused 370 μm under the sample surface using a NA = 0.6 objective while the probe was translated with a constant speed of 6 cm min^{-1} by high-precision bearing stages (ALS130, Aerotech Inc.). The mode field diameter of the guided modes was 22 μm × 22 μm at 789 nm. Propagation loss was measured at 0.3 dB cm^{-1} and birefringence was measured to be in the order of $B = 1 \times 10^{-7}$. Measured coupling with the input fibres (850 nm polarization-maintaining fibres, OZ Optics) was –6.7 dB, while losses at the output facet (graded-index multimode with 50 μm core diameter) were negligible.

Received 12 December 2012; accepted 22 March 2013; published online 12 May 2013

References

1. Nielsen, M. A. & Chuang, I. L. *Quantum Computation and Quantum Information* (Cambridge Univ. Press, 2000).
2. Ladd, T. D. *et al.* Quantum computers. *Nature* **464,** 45–53 (2010).
3. Knill, E. & Laflamme, R. Power of one bit of quantum information. *Phys. Rev. Lett.* **81,** 5672–5675 (1998).
4. Aaronson, S. & Gottesman, D. Improved simulation of stabilizer circuits. *Phys. Rev. A* **70,** 052328 (2004).
5. Jordan, S. P. Permutational quantum computing. *Quant. Infor. Comput.* **10,** 470–497 (2010).
6. Aaronson, S. & Arkhipov, A. in *Proceedings of the 43rd Annual ACM Symposium on Theory of Computing* 333–342 (ACM, 2011).
7. Gasparoni, S., Pan, J-W., Walther, P., Rudolph, T. & Zeilinger, A. Realization of a photonic controlled-NOT gate sufficient for quantum computation. *Phys. Rev. Lett.* **93,** 020504 (2004).
8. Okamoto, R., O'Brien, J., Hofmann, H. & Takeuchi, S. Realization of a Knill–Laflamme–Milburn controlled-NOT photonic quantum circuit combining effective optical nonlinearities. *Proc. Natl Acad. Sci. USA* **108,** 10067–10071 (2011).
9. Prevedel, R. *et al.* High-speed linear optics quantum computing using active feed-forward. *Nature* **445,** 65–69 (2007).
10. Metcalf, B. J. *et al.* Multiphoton quantum interference in a multiport integrated photonic device. *Nat. Commun.* **4**, 1356 (2013).
11. Spagnolo, N. *et al.* Three-photon bosonic coalescence in an integrated tritter. Preprint at http://lanl.arxiv.org/abs/1210.6935 (2012).
12. Spagnolo, N. *et al.* Quantum interferometry with three-dimensional geometry. *Sci. Rep.* **2,** 862 (2012).
13. Rohde, P. P. & Ralph, T. C. Error tolerance of the boson-sampling model for linear optics quantum computing. *Phys. Rev. A* **85,** 022332 (2012).
14. Knill, E., Laflamme, R. & Milburn, G. J. A scheme for efficient quantum computation with linear optics. *Nature* **409,** 46–52 (2001).
15. Gao, W. *et al.* Teleportation-based realization of an optical quantum two-qubit entangling gate. *Proc. Natl Acad. Sci. USA* **107,** 20869–20874 (2010).
16. Yoran, N. & Reznik, B. Deterministic linear optics quantum computation with single photon qubits. *Phys. Rev. Lett.* **91,** 037903 (2003).
17. Nielsen, M. A. Optical quantum computation using cluster states. *Phys. Rev. Lett.* **93,** 040503 (2004).
18. Browne, D. E. & Rudolph, T. Resource-efficient linear optical quantum computation. *Phys. Rev. Lett.* **95,** 010501 (2005).
19. Ralph, T. C., Hayes, A. J. F. & Gilchrist, A. Loss-tolerant optical qubits. *Phys. Rev. Lett.* **95,** 100501 (2005).
20. O'Brien, J. L., Furusawa, A. & Vuckovic, J. Photonic quantum technologies. *Nature Photon.* **3,** 687–695 (2009).
21. Aaronson, S. A linear-optical proof that the permanent is #**P**-hard. *Proc. R. Soc. A* **467,** 3393–3405 (2011).
22. Hong, C. K., Ou, Z. Y. & Mandel, L. Measurement of subpicosecond time intervals between two photons by interference. *Phys. Rev. Lett.* **59,** 2044–2046 (1987).
23. Zeilinger, A. General properties of lossless beam splitters in interferometry. *Am. J. Phys.* **49,** 882–883 (1981).
24. Arkhipov, A. & Kuperberg, G. The bosonic birthday paradox. *Geom. Topol. Monog.* **18,** 1–7 (2012).
25. Itoh, K., Watanabe, W., Nolte, S. & Schaffer, C. Ultrafast processes for bulk modification of transparent materials. *MRS Bull.* **31,** 620–625 (2006).
26. Marshall, G. *et al.* Laser written waveguide photonic quantum circuits. *Opt. Express* **17,** 12546–12554 (2009).
27. Reck, M. *et al.* Experimental realization of any discrete unitary operator. *Phys. Rev. Lett.* **73,** 58–61 (1994).
28. Kwiat, P. G. *et al.* New high-intensity source of polarization-entangled photon pairs. *Phys. Rev. Lett.* **75,** 4337–4341 (1995).
29. Laing, A. & O'Brien, J. L. Super-stable tomography of any linear optical device. Preprint at http://lanl.arxiv.org/abs/1208.2868 (2012).
30. Spring, J. B. *et al.* Boson sampling on a photonic chip. *Science* **339,** 798–801 (2013).
31. Broome, M. A. *et al.* Photonic boson sampling in a tunable circuit. *Science* **339,** 794–798 (2013).
32. Crespi, A. *et al.* Experimental boson sampling in arbitrary integrated photonic circuits. *Nature Photon.* http://dx.doi.org/10.1038/nphoton.2013.112 (in the press); preprint at http://lanl.arxiv.org/abs/1212.2783 (2012).

Acknowledgements

The authors thank S. Aaronson, Č. Brukner and M. Ringbauer for discussions. The authors acknowledge support from the European Commission under projects 'Q-ESSENCE—Quantum Interfaces, Sensors, and Communication based on Entanglement' (no. 248095), 'QuILMI—Quantum Integrated Light Matter Interface' (no. 295293) and the ERA-Net CHIST-ERA project 'QUASAR—Quantum States: Analysis and Realizations', the German Ministry of Education and Research (Center for Innovation Competence program, grant no. 03Z1HN31), the John Templeton Foundation, the Vienna Center for Quantum Science and Technology (VCQ), the Austrian Nano-initiative 'Nanostructures of Atomic Physics (NAP-PLATON)' and the Austrian Science Fund (FWF) under projects 'SFB-FoQuS—Foundations and Applications of Quantum Science', 'PhoQuSi—Photonic Quantum Simulators (Y585-N20)' and the doctoral programme 'CoQuS—Complex Quantum Systems', the Vienna Science and Technology Fund (WWTF; under grant no. ICT12-041), and the Air Force Office of Scientific Research, Air Force Material Command, United States Air Force (grant no. FA8655-11-1-3004).

Author contributions

M.T. designed and carried out the experiment, analysed data and waveguide structures, and wrote the manuscript. B.D. provided the theoretical analysis, analysed data and waveguide structures, and wrote the manuscript. R.H. designed and prepared the waveguide structures. S.N. and A.S. supervised the design and preparation of the waveguide structures. P.W. supervised the project, designed the experiment and wrote the manuscript.

Additional information

Supplementary information is available in the online version of the paper. Reprints and permissions information is available online at www.nature.com/reprints. Correspondence and requests for materials should be addressed to M.T. and P.W.

Competing financial interests

The authors declare no competing financial interests.